Preparation and Performance of Structure Controllable Biochar Obtained From Cattail-Sludge Composites

Fanfan Liang
Southwest Forestry University
Yan Wang (wycaf@126.com)
Southwest Forestry University

Research Article

Keywords: structure controllable, biochar, N, P, adsorption

Posted Date: September 7th, 2021

DOI: https://doi.org/10.21203/rs.3.rs-850268/v1

Abstract

Biochar obtained from cattail-sludge composites (BC/CS) was treated as a raw material, with monopotassium phosphate and ammonium chloride solution as absorbents, to find the best parameters for the preparation of structure controllable biochar (BC/SC). Slow pyrolysis and single factor experiment method were employed in the preparation of BC/CS and BC/SC, with EA, BET and SEM to illustrate the performance of BC/SC. The results showed that the best parameters for BC/CS were characterized by a ratio of cattail-sludge composites (60:40, wt%), a charring temperature of 500°C, a charring time of 0.5 hrs, KOH as an activator, an immersion ratio of 4 $mL \cdot g^{-1}$, an activation concentration of 300 $g \cdot L^{-1}$ and an immersion time of 6 hrs; the best parameters for BC/SC contained a sizing amount of 60%, a molding pressure, temperature and time of 5 N $(cm^2)^{-1}$, 160°C, and 95 min, respectively; compared to BC/CS, BC/SC was characterized by a higher content of H but a lower O content, leading to the increase in its hydrophobicity and stability; in addition, the addition of polyethylene enabled an increase in the pore diameter of BC/SC and a close bond with particles on the surface. Meanwhile, in BC/SC, the surface functional groups of CH3 and C—O—C were reduced in their contents, in contrast to a large amount of C crystals on its surface. Such results could provide a new process for resource recycling of cattail and sludge, as well as evidence for material selection in the treatment of eutrophication water bodies.

Introduction

In contrast to the severe shortage of phosphorous (P) resources worldwide, large amounts of N and P have been discharged into surface water bodies due to large-scale agricultural and industrial production, resulting in eutrophication in water bodies[1]. Additionally, the discharge of N and P in large amounts has led to anoxia, fish deaths, and destruction of water ecosystems and even to dangers such as toxic algae[2,3]. The removal and recycling of N and P in water is of great significance to mitigate agricultural and ecological crises [4]. Extensive studies have been performed on the technologies of N and P removal in water bodies, mainly involving precipitation[5], film technology[6], reverse osmosis[7], coagulation[8], flocculation[9], catalytic reduction[10], and adsorption[11]. Among them, adsorption is a more efficient and selective technology for N and P removal. Biochar is an excellent absorbent, low in solubility, rather large in porosity and BET surface area, rich in negative charge on the surface, high in charge density, and strong in stability[12]. However, in practice, there are still some disadvantages of powder biochar, among which the most important is its difficulty in separation and recycling during waste treatment and even in secondary powder pollution. Considering this, BC/SC of a certain size and strength can overcome such demerits.

Cattails are commonly used aquatic macrophytes for wetland ecosystem restoration. Its stalks are mainly foliage, with large spongy pores between cells[13]. Biochar obtained from cattail can avoid secondary pollution from its decomposition and be an absorbent to remove N and P in the water[14,15]. Sludge, if disposed of as solid waste, is of great harm to the environment, including harms such as organic pollution and pollution from pathogenic microorganisms[16,17]. Biochar from sludge through pyrolysis can not only completely kill both parasite eggs and pathogenic microorganisms but also achieve carbon sequestration[18]. In this study, BC/CS was selected as the raw material to find the best parameters for the preparation of BC/SC. EA, BET, and SEM were employed to illustrate the performance of BC/SC in hope of providing a new process for resource utilization of cattail and sludge, as well as evidence for material selection in the treatment of eutrophication water bodies.

1. Materials And Methods

1.1 Biochar preparation

Aquatic macrophyte cattail and sludge were selected as the raw materials. In August 2020, cattail and sludge were collected in the ditch along Nanyuan Road of the branch of the Jizhi River, the upper reach of Dianchi Lake. Slow pyrolysis was employed, and parameters were set (see Table 1) to select the best one for BC/CS through pyrolysis to determine methods for biochar preparation. KOH (300 $g \cdot L^{-1}$) was combined with a mixture of cattail and sludge (60:40, wt%) at an immersion ratio of 4 $mL \cdot g^{-1}$. After 6 h of oscillation (THZ-Q, desktop frozen thermostatic oscillator), it was put into a muffle furnace (ELF-11-14B muffle) and carbonized for 0.5 h at 500℃ after an increase in temperature at a rate of 10℃$\cdot min^{-1}$. Then, it was ground, filtered through a 60 mesh and stored in a dry container for later use.

1.2 Preparation of BC/SC

A 2*2*2 cm cube BC/SC were prepared by BC/CS. A single factor experiment method was employed to select the best parameters for BC/SC and thus to determine its preparation methods (see Table 2). A high-density polyethylene (200 mesh) was fully mixed with BC/CS at a ratio of 3:2 on the basis of its weight, and then the mixture was first molded under a pressure of 5 $N \cdot (cm^2)^{-1}$ in a mold, formed in the cold after 95 min of heating at 160℃, and kept in a dry container for later use. The molding and mechanical strength testing device of BC/SC was established according to Fig. 1. The molding pressure and mechanical strength were calculated according to the expression below:

$F=m*9.8N \cdot kg^{-1}/4\ cm^2$

where F refers to the molding pressure and mechanical strength $N \cdot (cm^2)^{-1}$, m refers to the weight, kg, 9.8 $N \cdot kg^{-1}$ refers to the gravitational acceleration, and4 cm^2 refers to the pressed area.

1.3 Performance of BC/SC

The surface morphology of BC/SC was scanned by an American FEIQ45 scanning electron microscope (SEM), the content of C, H, O and N was determined by PE SERIES II 2400 element analyzer (EA), and the BET surface area was determined by American Quadra Sord EVA. Its surface crystal was determined by a Japan X-ray diffractometer (2550 VB/PC X), and its functional groups were determined by an American Fourier Transform Infrared Spectrometer (Thermo Scientific Nicoler IS5).

2. Results And Discussions

2.1 Process for the preparation of BC/CS

With the increase in the portion of cattail, N and P adsorption first increased and then decreased (see Fig. 2a). Compared with 0% cattail addition, 20% cattail addition significantly increased N and P adsorption on biochar, and 60% cattail addition showed the most N and P adsorption, with N adsorption 0.4407 $mg \cdot g^{-1}$ more than P adsorption. Zhang et al.[19] egreed rice rust sludge biochar through copyrolysis; thus, it is supposed that biochar with 60% cattail addition possesses a rather optimized structure. Considering its N and P adsorption capacity, 60% cattail addition was selected as the process parameter for cattail addition.

The great difference in charring temperature in N and P adsorption is shown in Fig. 2b. Compared with N adsorption, P adsorption increased by 1.6707 $mg \cdot g^{-1}$ at 500°C. N adsorption was greatly affected by temperature. At 400°C, N adsorption on the charring biochar was 2.1577 $mg \cdot g^{-1}$ higher than that at 300°C. At 500°C, N and P adsorption reached the peak. This result was similar to the research of Wang et al.[20], who found that the best charring temperature of sludge straw biochar through copyrolysis was 503.19°C. Shi et al.[21] also reported that sludge biochar possessed the best P adsorption capacity at 700°C. Thus, it is estimated that the biomass of plants shows good modification to sludge biochar and reduces the temperature requirement for the preparation of sludge biochar.

The effects of charring time on N and P adsorption also showed great differences (Fig. 2c). With increasing charring time, N adsorption first decreased and then increased afterward, in contrast to a decrease in P adsorption. P adsorption on biochar after 8 h of charring decreased significantly. Different charring times showed great differences in N and P adsorption. After 0.5 h of charring, the difference in N and P adsorption equaled 1.9232 $mg \cdot g^{-1}$. Wang et al.[22] prepared biochar from cattail and phragmites with a 20 min charring time, in addition to a sludge biochar preparation with a 15 min charring time by Mao et al.[23]. Given N and P adsorption, 0.5 h was selected as the process parameter for charring time.

The effect of the activator on N was similar to that on P, but a large difference in adsorption occurred, as shown in Fig. 2d. With potassium hydroxide as an activator, P adsorption on the biochar was 3.0535 $mg \cdot g^{-1}$ higher than N adsorption. N adsorption was greatly affected by the types of activators. N adsorption with potassium hydroxide as an activator was 1 $mg \cdot g^{-1}$ higher than that with zinc chloride and phosphoric acid. Studies have shown that biochar with potassium hydroxide as an activator possesses excellent structures, such as a large BET surface area and rich pores, and biochar with potassium hydroxide as an activator also shows good N and P adsorption[24]. Thus, potassium hydroxide was selected as the process parameter for the activator type.

As shown in Fig. 2e, the effects of the immersion ratio on N adsorption were similar to those on P adsorption; both tended to rise first and then decrease. The immersion ratio showed a greater effect on N adsorption. The difference between N and P adsorption on biochar with an immersion ratio of 4 $mL \cdot g^{-1}$ was 2.2580 $mg \cdot g^{-1}$. Potassium hydroxide was used as an activator to obtain biochar from mushroom residue[25]and water chestnut shells[26]at a mass ratio of 4:1, and the results of N and P adsorption on biochar were similar to the largest N and P adsorption in this study at an immersion ratio of 4 $mL \cdot g^{-1}$. Accordingly, 4 $mL \cdot g^{-1}$ was selected as the process parameter for the immersion ratio.

As shown in Fig. 2f, the effects of activator concentrations on N and P adsorption were similar. If the concentration was less than 300 $mg \cdot L^{-1}$, N and P adsorption rose rapidly and then decreased slowly. A great difference occurred between the effects of activator concentrations on N and P adsorption. Their difference reached 0.7571 $mg \cdot g^{-1}$ at a concentration of 300 $mg \cdot L^{-1}$. The rise in the activator concentration significantly inhibited N adsorption. At activator concentrations of 400 and 900 $mg \cdot L^{-1}$, N adsorption on biochar reached 8.6089 and 5.9588 $mg \cdot g^{-1,}$ respectively. In light of the effects of different activator concentrations on N and P adsorption on biochar, 300 $mg \cdot L^{-1}$ was selected as the process parameter for activator concentration.

As shown in Fig. 2g, immersion time showed no significant impact on P adsorption, in contrast to a rather large impact on N adsorption. The 6-8 h immersion time significantly increased N adsorption, in contrast to decreased P

adsorption. Studies have shown the large impacts of activator concentrations on immersion time. If there was a high activator concentration, then the immersion time was short, and vice versa. Song et al.[27] obtained biochar with potassium hydroxide as an activator at a concentration of 1 g·mL^{-1} for 12 h, in contrast to a 15% concentration of potassium hydroxide for 4 h by Guo et al.[28]. Considering the effects of immersion time on N and P adsorption, 6 h was determined as the process parameter for immersion time.

2.2 Process for the preparation of BC/SC

2.2.1 Impacts of sizing amounts on BC/SC

The impacts of sizing amounts on N and P adsorption on BC/SC were similar (Fig. 3); both decreased first and then increased afterward. The increase in the content of polyethylene inhibited N adsorption on BC/SC, especially when sizing amounts reached 40% and 50%, and the difference between N and P adsorption tended to be large. Meanwhile, with the increase in sizing amounts, the mechanical strength of controllable biochar rose, with little difference between N and P adsorption, which suggested a similar impact of the N and P solutions on BC/SC. It was found that only when the mechanical strength exceeded 100 N·(cm^2)$^{-1}$ could long-term water scouring and air shock occur[29]. Although the mechanical strength exceeded 100 N·(cm^2)$^{-1}$ with a sizing amount of 50%, in light of the complexity of the water environment and N and P adsorption, a 60% sizing amount was determined for the preparation of BC/SC.

2.2.2 Impacts of molding pressures on BC/SC

Different molding pressures showed different impacts on N and P adsorption on BC/SC (Fig. 4). With increasing molding pressure, P adsorption on BC/SC decreased gradually, whereas N adsorption rose first and then decreased afterward. This result indicated that polyethylene played a role in the modification of BC/CS, leading to some changes in the physical and chemical properties of BC/CS and strengthening N adsorption, which was proven in the performance of BC/CS. The mechanical strength of BC/SC increased with molding pressure and reached more than 140 N·(cm^2)$^{-1}$ under a molding pressure of 5 N·(cm^2)$^{-1}$. In light of the complexity of the water environment and N and P adsorption, a molding pressure of 5 N·(cm^2)$^{-1}$ was determined for BC/SC preparation.

2.2.3 Impacts of molding temperature on BC/SC

A similar tendency occurred between the impacts of molding temperatures on N and P adsorption on BC/SC (Fig. 5). Both N and P adsorption rose first and decreased later. N and P adsorption reached their peaks at temperatures of 155°C and 160°C, respectively. When it rose from 155℃ to 160℃, P adsorption rose significantly. This result suggested that increasing the temperature to a certain point promoted the modification of BC/CS by polyethylene and strengthened P adsorption. Below 160℃, increasing the temperature enhanced the mechanical strength of BC/SC. When the temperature exceeded 160℃, its mechanical strength decreased significantly. This result indicated that temperatures beyond a certain point showed a strong negative effect on the structure. In light of N and P adsorption and mechanical strength, a temperature of 160℃was determined for the preparation of BC/SC.

2.2.4 Impacts of forming time on BC/SC

The impacts of different forming times on the N and P adsorption of BC/SC were similar (Fig. 6). Both N and P adsorption rose first and later decreased. Generally, a significant difference occurred between the N and P

adsorption of BC/SC. This result indicated different roles of biochar composition in BC/SC N and P adsorption capacity, and a certain prolonged forming time would strengthen its N and P adsorption capacity. Too long of a forming time led to a decrease in N and P adsorption on BC/SC, as well as in mechanical strength. This illustrated the destruction of polyethylene on its structure, leading to a decrease in its mechanical strength. Considering N and P adsorption and mechanical strength, a forming time of 95 minwas determined for the preparation of BC/SC.

2.3 Performance of BC/SC

2.3.1 Element content, BET surface area and pore structure

The contents of C and H in BC/SC were higher than those in BC/CS, but the O content was lower (Table 3). The reason can be ascribed to the addition of polyethylene (with a simplified structure -[-CH2-CH2-]n-), which led to a significant increase in its content of C and H and a decrease in its content of O. The lower the content of functional groups containing O was, the stronger the hydrophobicity of the biochar was[29]. The O/C value of BC/SC was far lower than that of BC/CS. This result indicated that the hydrophobicity of BC/SC was stronger than that of BC/CS. This might be attributed to the hydrophobicity resulting from the addition of polyethylene. The values of H/C and O/C could reflect biochar stability, and low values show an aromatic ring structure and strong stability of biochar[31]. It is generally believed that the most stable biocha should have an O/C value less than 0.2[32]. The O/C value of BC/SC, 0.17, was lower than that of BC/CS. Thus, it suggested a rather strong stability of BC/SC, its ability to exist in the environment for a long time, and great potential for eutrophicated water pollution treatment. The lower the (O+H)/C value was, the lower the biochar polarity was[8]. Accordingly, the polarity of BC/SC was lower than that of BC/CS. In summary, the addition of polyethylene changed the elemental composition of BC/CS and impacted the physical and chemical properties of BC/CS, making BC/SC different from BC/CS in terms of surface functional groups, hydrophilia or hydrophobicity, and stability.

The BET surface area (S_{BET}) of BC/SC was significantly lower than that of BC/CS (Table 4). This result indicated the full combination of polyethylene and BC/CS. There was little difference in the surface area of micropores (S_{mic}) between BC/SC and BC/CS. Considering the important role of micropores in biochar adsorption of pollutants, BC/SC still possessed the capacity of pollution adsorption. A large difference occurred between BC/SC and BC/CS in pore volume (V_{pore}) and micropore volume (V_{mic}), also indicating the full combination of polyethylene and BC/CS. The average pore diameter (D_{pore}) of BC/SC was similar to that of BC/CS, indicating no significant impacts of polyethylene addition on the average pore diameter. In sum, the addition of polyethylene greatly impacted the pore structure of BC/CS.

BC/SC was characterized by a coarse surface, abundant particles and loose dispersal, indicating a significant change in surface morphology. The addition of polyethylene enabled a close bond with BC/CS particles. Its particles were obvious, with increased coarseness, and pore diameters of different sizes were clearly visible with obvious filmy materials (Fig. 7). Considering the large amount of C crystals on the surface of BC/CS, it was suggested that the film materials were mainly formed by C crystals.

2.3.3 Surface functional groups and surface crystals

The adsorption of BC/SC reached a peak near BC/SC, illustrating the existence of —OH (Fig. 8). In contrast, the peak strength of BC/CS was just slightly weaker, suggesting no significant impact of polyethylene addition on the

surface OH functional groups of BC/CS. CH_3 appeared at the absorption peak near 1455.06 cm^{-1}, in contrast to a C—O—C oscillation near 1016.51 cm^{-1}. In comparison to BC/CS, the peak strength of BC/SC was weaker, and a significant decrease in C—O—C functional groups was observed. Near 694.39 cm^{-1}, an adsorption peak was observed on BC/CS, illustrating the existence of a benzene ring, while no adsorption peak was observed on this site on BC/SC. This result indicated that polyethylene addition inhibited functional groups on the surface of BC/CS. Consequently, polyethylene addition played a negative role in the surface functional groups of BC/CS.

The surface of BC/CS was rich in SiO_2 crystals, in contrast to the richness in $C_{23}H_{48}$ and reduction in SiO_2 and Na_3CrO_4 in BC/SC, which indicated the full coverage of polyethylene on the surface of BC/CS (Fig. 9). No material containing K was observed on the surface of BC/CS and BC/SC after the addition of KOH as an activator, which suggested that the spillover effects of metallic ions can be avoided during environmental treatment through BC/SC. BC/SC contained 38.5% of C crystals. After a comparison with the BC/CS results through SEM, it is suggested that the film materials on BC/SC were mainly C crystals. Considering that film materials were mainly observed on the edge of pores, it was inferred that the formation of film materials occurred during the flow of polyethylene with C crystals wrapped at the molding temperature.

3. Conclusions

(1) The best parameters for the preparation of BC/CS were characterized by a ratio of cattail-sludge composites (60:40, wt%), a 500℃ charring temperature, 0.5 charring hrs, KOH as an activator, a 4 $mL \cdot g^{-1}$ immersion ratio, a 300 $g \cdot L^{-1}$ activation concentration and 6 hrs of immersion.

(2) The best parameters for the preparation of BC/SC were a sizing amount of 60%, a molding pressure of 5 N $(cm^2)^{-1}$, a molding temperature at 160℃, and a forming time of 95 min.

(3) In comparison with BC/CS, BC/SC contained more H content and less O content, which promoted its hydrophobicity and stability. The polyethylene addition increased its pore diameter and made a close bond between particles on the surface. It involves less content of —CH3 and C—O—C functional groups, but a large amount of C crystals on its surface.

Declarations

Acknowledgements

This work was supported financially by the National Natural Science Foundation of China (41761098,21767027).

Author contributions

Fanfan Liang: Investigation, Writing-original draft, Formal analysis, Visualization, Software, Methodology. **Yan Wang:** Conceptualization, Methodology, Writing-review & editing, Supervision, Data curation.

Declaration of Competing Interest

The authors declare that they have no known competing financial interests or personal relationships that could have appeared to influence the work reported in this paper.

References

1. Pu, J. *et al.* Implications of phosphorus partitioning at the suspended particle-water interface for lake eutrophication in China's largest freshwater lake, Poyang Lake. Chemosphere (Oxford). 263, 128334(2021).
2. Ahmed, S. & Lo, I. M. C. Phosphate removal from river water using a highly efficient magnetically recyclable Fe3O4/La(OH)3 nanocomposite., **261**, 128118 (2020).
3. Yang, Y. *et al.* Great enhancement in phosphate uptake onto lanthanum carbonate grafted microfibrous composite under a low-voltage electrostatic field., **264**, 128378 (2021).
4. Xu, W. *et al.* Using iron ion-loaded aminated polyacrylonitrile fiber to efficiently remove wastewater phosphate. *Chem Eng J*, **403**, 126349 (2021).
5. Quan, X., Ye, C., Xiong, Y., Xiang, J. & Wang, F. Simultaneous removal of ammonia, P and COD from anaerobically digested piggery wastewater using an integrated process of chemical precipitation and air stripping. *J Hazard Mater*, **178**, 326–332 (2010).
6. van Voorthuizen, E. M., Zwijnenburg, A. & Wessling, M. Nutrient removal by NF and RO membranes in a decentralized sanitation system. *Water Res*, **39**, 3657–3667 (2005).
7. Karami, P., Khorshidi, B., Soares, J. B. P. & Sadrzadeh, M. Fabrication of Highly Permeable and Thermally Stable Reverse Osmosis Thin Film Composite Polyamide Membranes. *Acs Appl Mater Inter*, **12**, 2916–2925 (2019).
8. Liao, P. *et al.* Adsorption of nitrogen-heterocyclic compounds on bamboo charcoal: Kinetics, thermodynamics, and microwave regeneration. *J Colloid Interf Sci*, **390**, 189–195 (2013).
9. Sadri Moghaddam, S., Alavi Moghaddam, M. R. & Arami, M. Coagulation/flocculation process for dye removal using sludge from water treatment plant: Optimization through response surface methodology. *J Hazard Mater*, **175**, 651–657 (2010).
10. Yang, G. C. C. & Lee, H. Chemical reduction of nitrate by nanosized iron: kinetics and pathways. *Water Res*, **39**, 884–894 (2005).
11. Perumal, K. & Sankaran, M. In-situ fabrication of zirconium entrenched biopolymeric hybrid membrane for the removal of toxic anions from aqueous medium.*Int J Biol Macromol*. 141, (2019).
12. Wang, C., Li, L., Shi, J. & Jin, H. Biochar production by coconut shell gasification in supercritical water and evolution of its porous structure. *J Anal Appl Pyrol*, **156**, 105151 (2021).
13. Hou, J. *et al.* BiOCl/cattail carbon composites with hierarchical structure for enhanced photocatalytic activity. *Sol Energy*, **211**, 1263–1269 (2020).
14. Bo, W., Fayun, L. & Li, W. Enhanced hexavalent chromium (Cr(VI)) removal from aqueous solution by Fe–Mn oxide-modified cattail biochar: adsorption characteristics and mechanism.*Chem Ecol*. 36, (2020).
15. Hou, J., Jiang, T., Wei, R., Idrees, F. & Bahnemann, D. Ultrathin-Layer Structure of BiOI Microspheres Decorated on N-Doped Biochar With Efficient Photocatalytic Activity. *Front Chem*, **7**, 378–378 (2019).
16. Kou, L., Wang, J., Zhao, L., Jiang, K. & Xu, X. Coupling of KMnO4-assisted sludge dewatering and pyrolysis to prepare Mn,Fe-codoped biochar catalysts for peroxymonosulfate-induced elimination of phenolic pollutants. *Chem Eng J*, **411**, 128459 (2021).
17. Chang, Y. C. *et al.* Transformation characteristics of polycyclic aromatic hydrocarbons during hydrothermal liquefaction of sewage sludge. *The Journal of Supercritical Fluids*, **170**, 105158 (2020).

18. Bao, D. *et al.* Metal-modified sludge-based biochar enhance catalytic capacity: Characteristics and mechanism. *J Environ Manage*, **284**, 112113 (2021).
19. Zhang, J., Diao, H. J. & Wang, M. Y. Effects of rice husk and sewage sludge co-prolysis on characteristics of the sludge biochar and its ecological risk of heavy matals. *Acta Sci. Circum*, **4**, 1250–1256 (2019).
20. Wang, Z. *et al.* Optimization of using co-pyrolysis of sludge and straw of prepare biochar and adsorption of Cr(â…¥). *Environmental Engineering*, **37**, 139–143 (2019).
21. Shi, C., Zhang, P., Guo, J. & Zhang, G. Phosphorus adsorption performance onto sewage sludge biochar. *Chinese Journal of Environmental Engingeering*, **10**, 7203–7208 (2016).
22. Wang, B., Ye, C., Li, F., Qu, Q. & Chen, X. Studies on adsorption of nitrate from modified hydrophyte biochars. *China Environmental Science*, **1**, 116–122 (2017).
23. Mao, K., Chen, H. M. & Chen, T. M. Adsorption effects of sludge biochar of different particle size on Zn contamination in water.*Acta Scientiae Circumstantiae*.884–894. (2020).
24. Yang, Q., Wang, C., Ren, N., Zhao, Z. & Wei, W. Study on the preparation and application of biochar. *Applied Chemical Industry*, **49**, 1836–1838 (2020).
25. Zhu, Y. *et al.* Effect of preparation conditions on the phosphorus adsorption capacities of modified biochar. *Ecology and Environmental Sciences*, **9**, 1897–1903 (2020).
26. Xiao, X. *et al.* Preparation and capacitive properties of water caltrop shell-based porous carbon for supercapacitor. *Functional Materials*, **50**, 12080–12084 (2019).
27. Song, Z., Shi, X. & Lin, Z. Synthesis and characterization of reed-based biochar and its adsorption properties for Cu2+ and bisphenol A (BPA). *Environ Chem*, **8**, 2196–2205 (2020).
28. Guo, J. *et al.* Preparation of Sludge-Based Biomass Carbon and Its Adsorption on Copper in Water. *HUNAN AGRICULTURAL SCIENCES*, **5**, 30–33 (2019).
29. Yu, X., Liu, Y. & Zhang, G. Study on Preparation and Performance of Formed Activaated Carbon with Deposited TiO2 Thin Films. *Anhui University of Technology*, **3**, 280–283 (2008).
30. Masebinu, S. O., Akinlabi, E. T., Muzenda, E. & Aboyade, A. O. A review of biochar properties and their roles in mitigating challenges with anaerobic digestion. *Renewable and Sustainable Energy Reviews*, **103**, 291–307 (2019).
31. Kuhlbusch, T. A. J. Method for Determining Black Carbon in Residues of Vegetation Fires. *Environ Sci Technol*, **29**, 2695–2702 (1995).
32. Spokas, K. A. Review of the stability of biochar in soils: predictability of O:C molar ratios. *Carbon Manag*, **1**, 289–303 (2014).

Tables

Table 1 Parameter setting of biochar preparation process

Mixing ratio %	0	15	30	45	60	75	90	100
Charring temperature ℃	200	300	400	500	600	700	800	
Charring time h	0.5	1	1.5	2	4	8		
Activator Type	potassium hydroxide			zinc chloride		phosphoric acid		
Immersion ratio mL·g^{-1}	0.5	1	1.5	2	3	4	5	
Activator concentration g·L^{-1}	50	100	150	200	300	400	500	700	900	1100
Immersion time h	2	4	6	8	10	12	16	20

Table 2 Parameter settings of the BC/SC preparation process

Sizing amount %	30	40	50	60	70
Molding pressure N·□cm^{2}□$^{-1}$	5	8	11	15	20
Molding temperature ℃	150	155	160	165	170
Forming time min	45	75	95	115	175

Table 3 Elemental content and atomic ratio of biochar

	w□C□/%	w□H□/%	w□O□/%	w□N□/%	O/C	H/C	□O+H□/C
BC/CS	9.45	0.57	15.30	<0.3	1.61	0.06	1.68
BC/SC	44.30	5.18	7.60	<0.3	0.17	0.12	0.29

Table 4 Biochar BET surface area, pore volume, and average pore diameter

	S_{BET}/m^2·g^{-1}	S_{mic}/m^2·g^{-1}	V_{pore}/cm^3·g^{-1}	V_{mic}/cm^3·g^{-1}	D_{pore}/nm
BC/CS	6.2063	0.7240	0.0276	0.0003	17.7673
BC/SC	0.4573	0.7391	0.0021	0.00008	18.7787

Figures

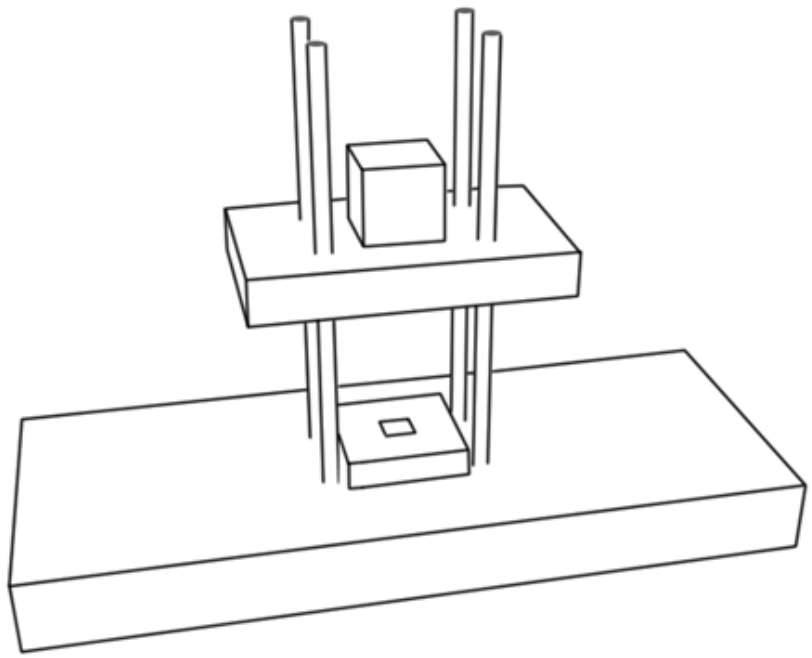

Figure 1

Schematic diagram of the BC/SC molding and mechanical strength testing device

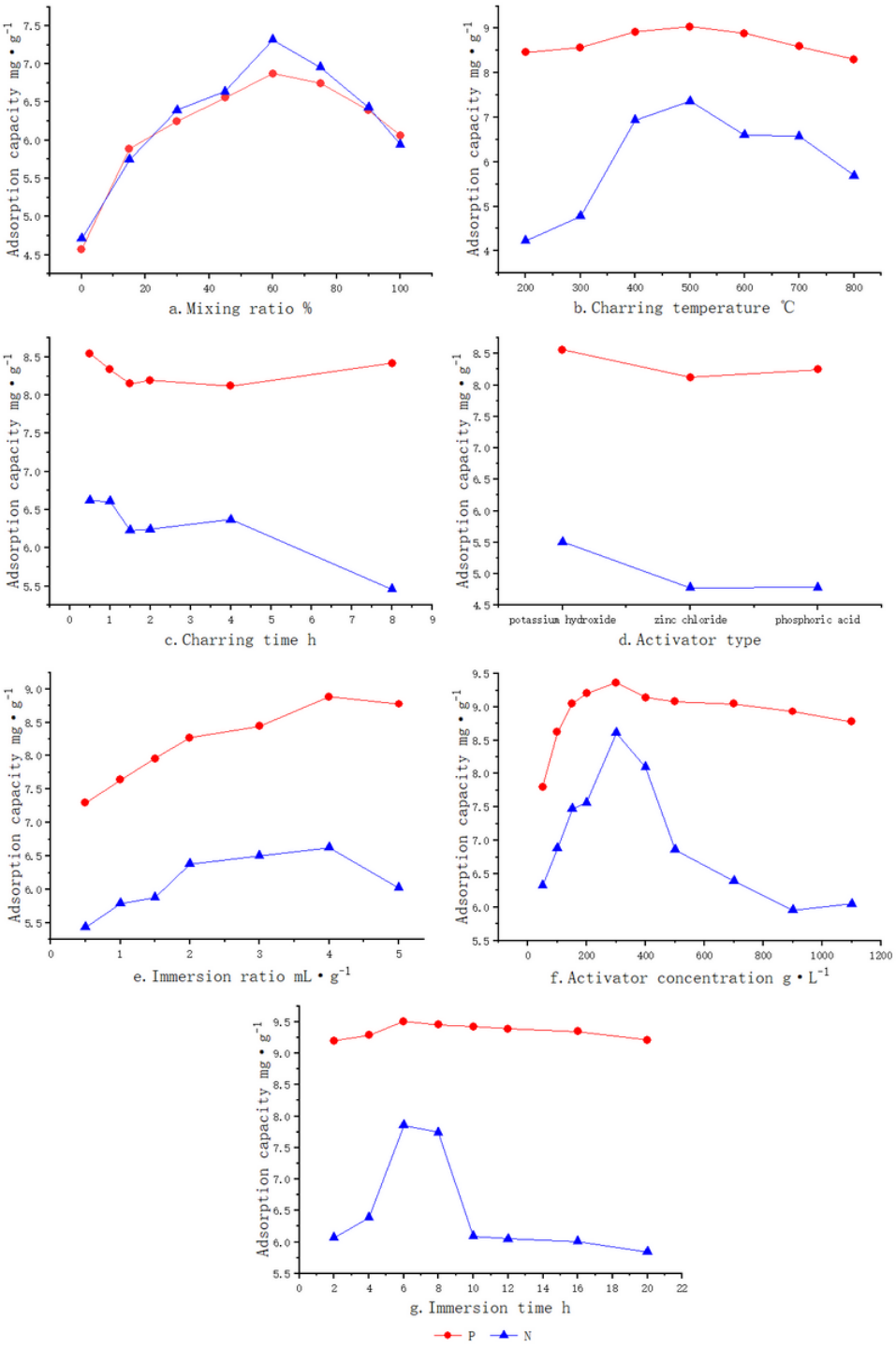

Figure 2

Biochar preparation process

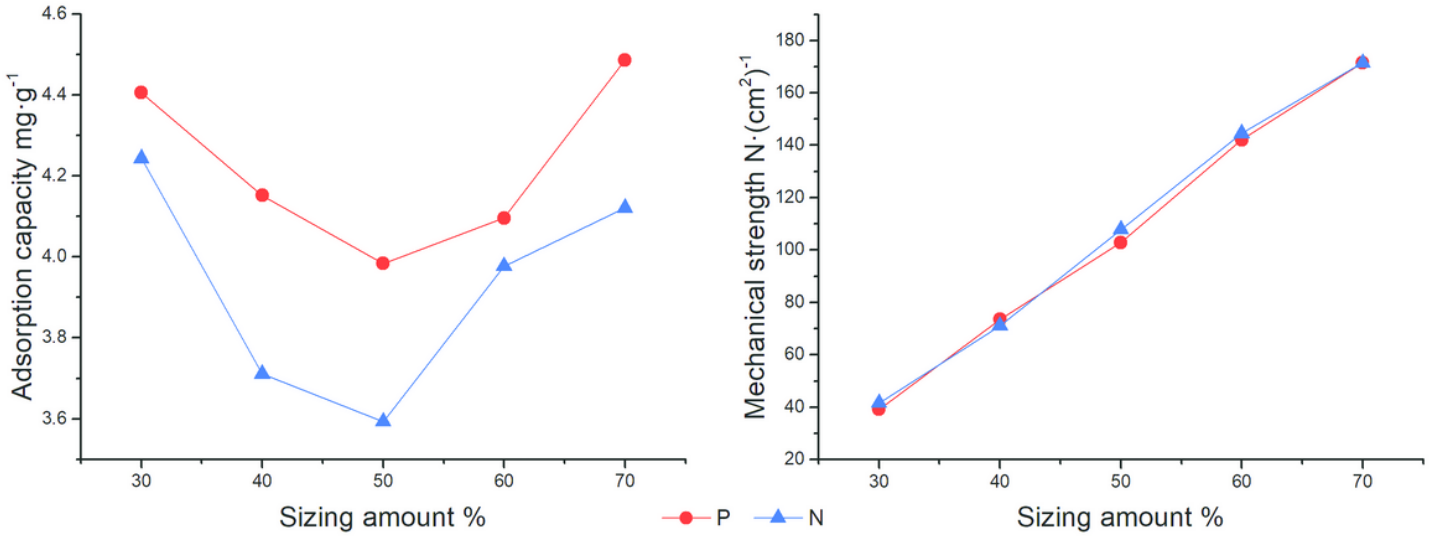

Figure 3

Nitrogen and phosphorus adsorption capacity and mechanical strength of controllable biochar with different sizing amounts

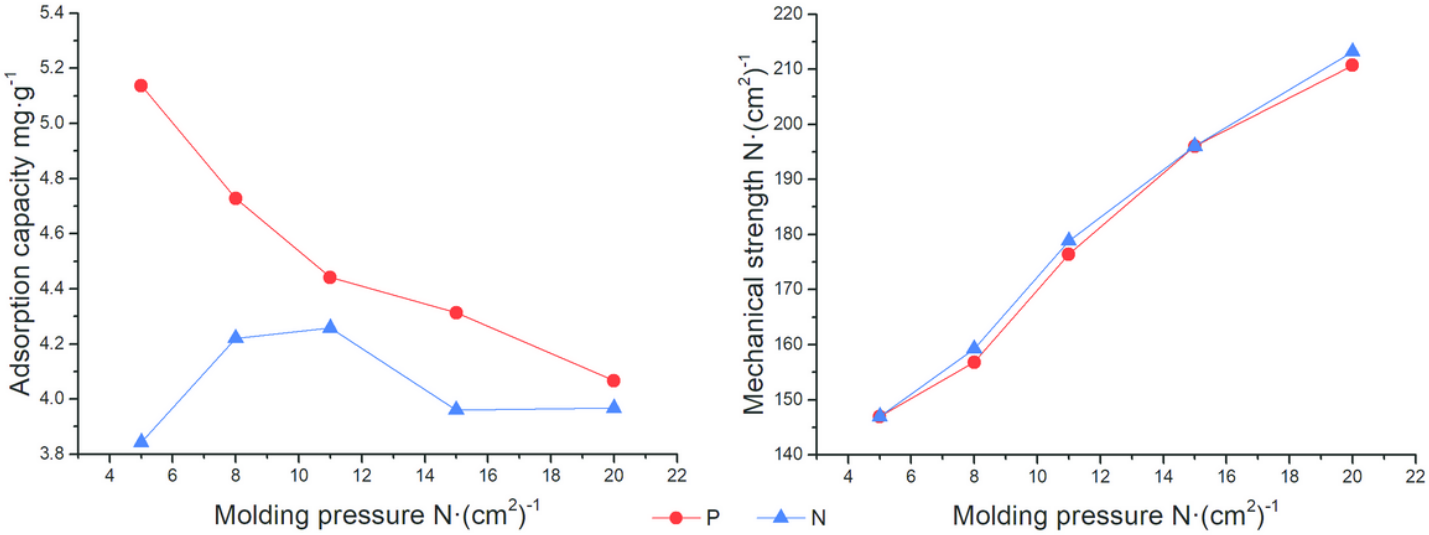

Figure 4

N and p adsorption capacity and mechanical strength of controllable biochar under different molding pressures

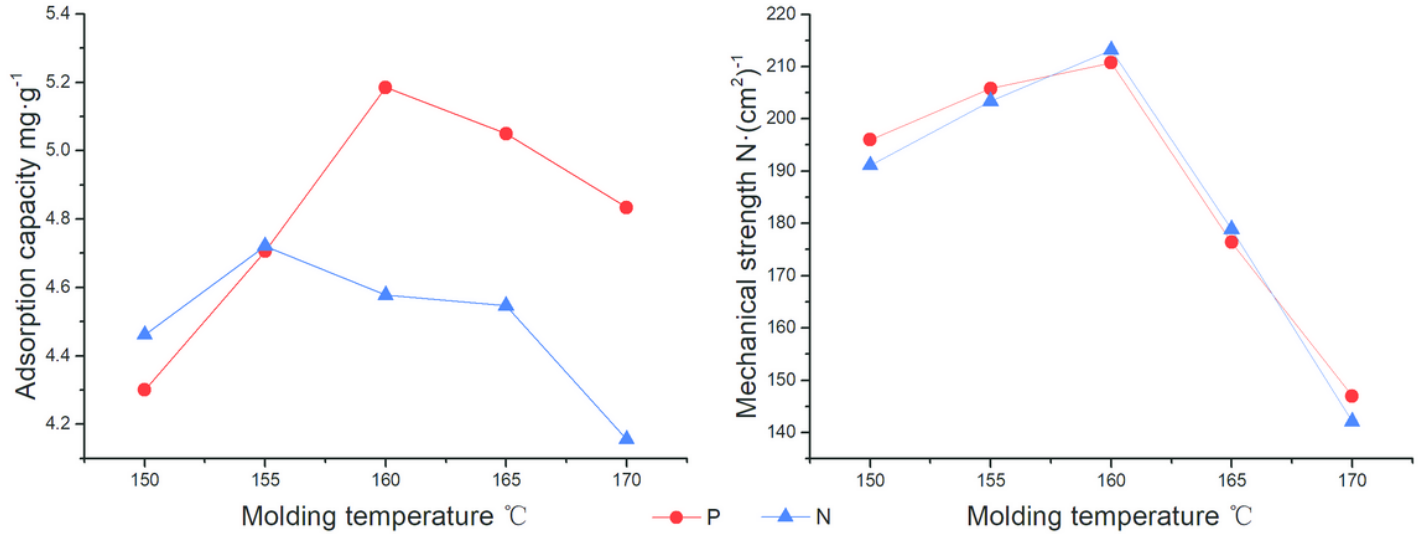

Figure 5

Nitrogen and phosphorus adsorption capacity and mechanical strength of controllable biochar at different molding temperatures

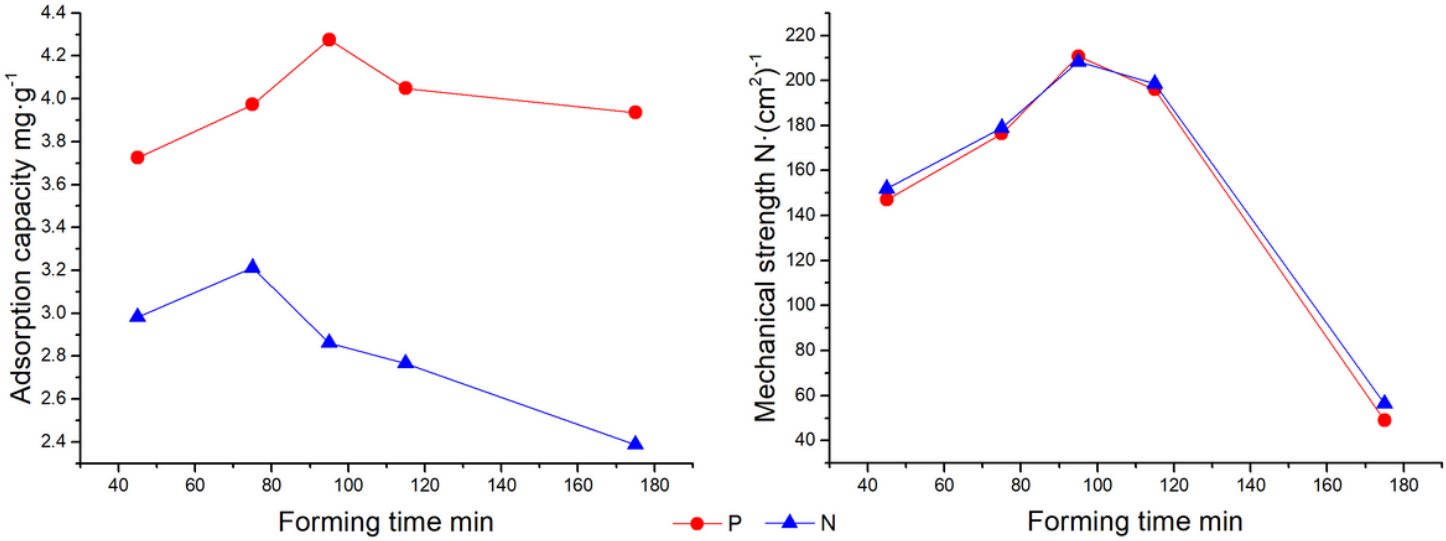

Figure 6

Nitrogen and phosphorus adsorption capacity and mechanical strength of controllable biochar at different forming times

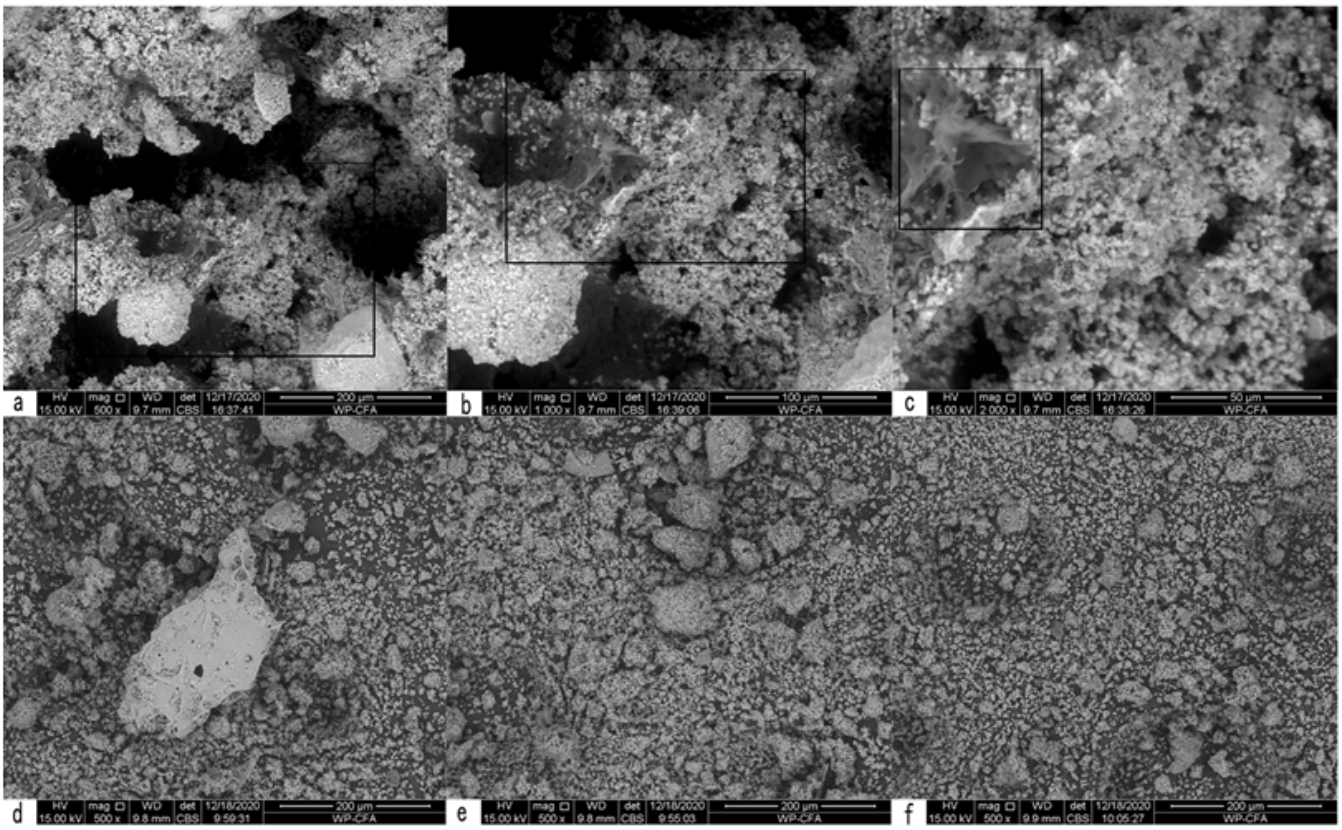

Figure 7

Surface morphology of structural biochar

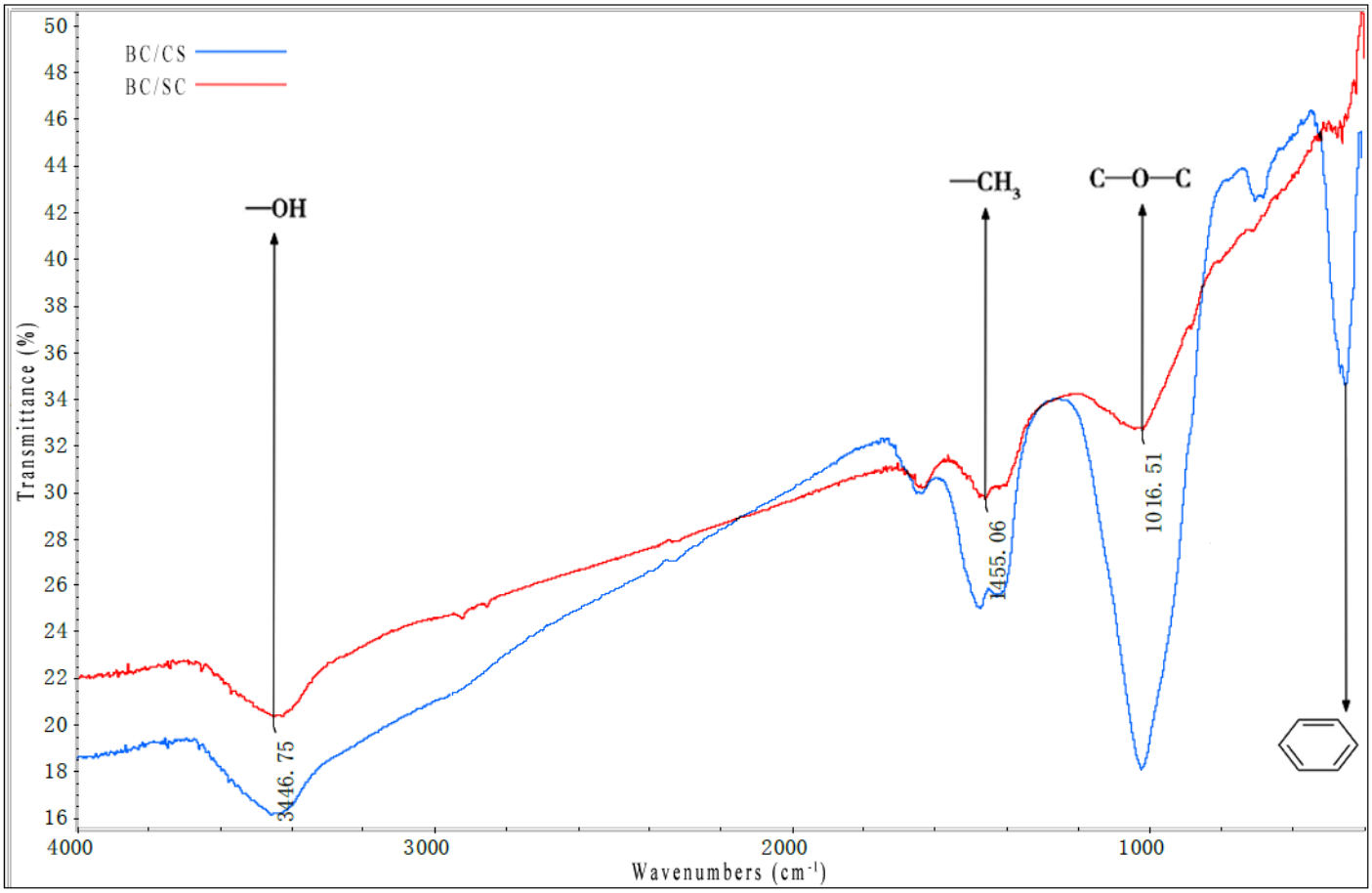

Figure 8

Surface functional groups of biochar

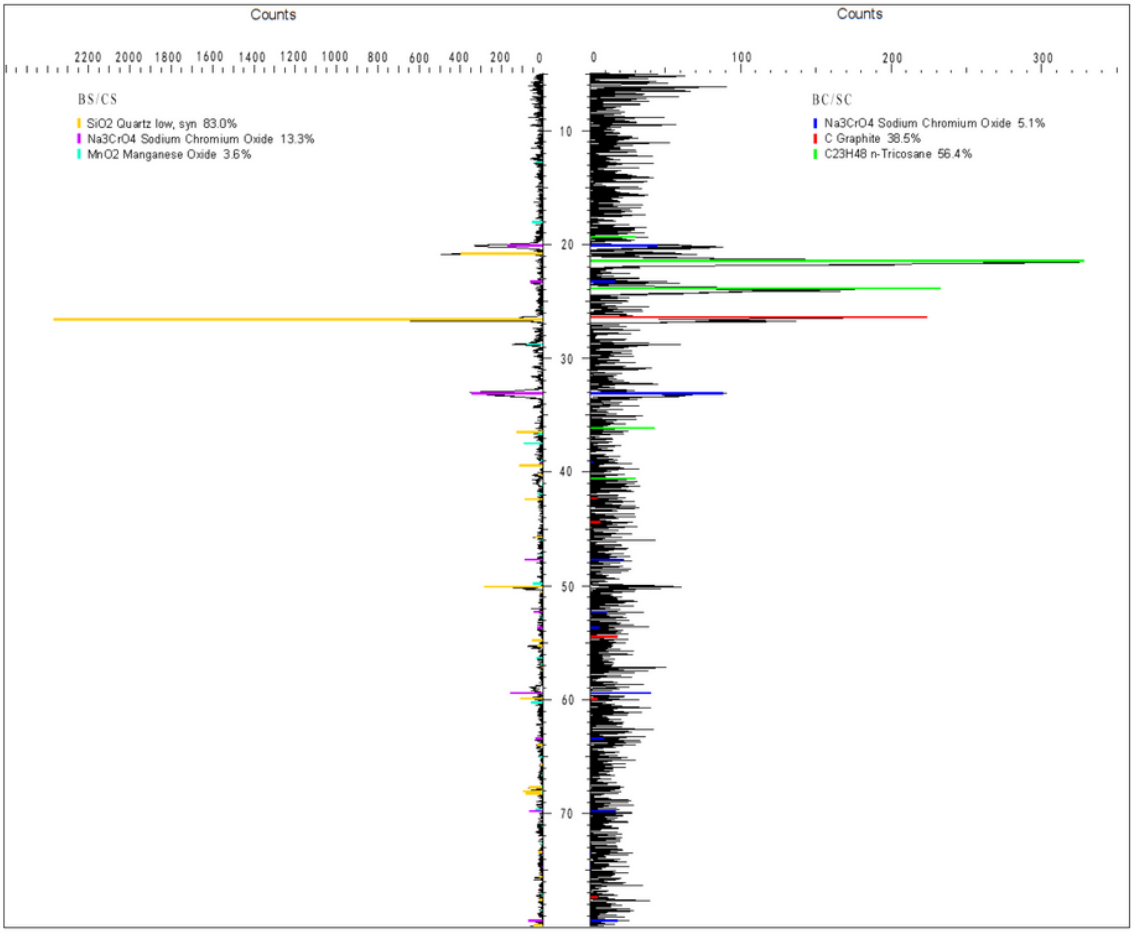

Figure 9

Surface crystals of biochar